Dynamic Analysis of Human Gait Cycle and Squat

Alexandra Santos[1], Diogo Marques[1], Filipa Baltazar[1] and Rita Martins[1]

[1] *Instituto Superior Técnico, Integrated Master's in Biomedical Engineering,*
{alexandrabettencourt, diogo.m.marques, a.filipa.baltazar, rita.r.martins.}@tecnico.ulisboa.pt

ABSTRACT — *Analogously to kinematic, dynamic analysis can play major roles in fields such as sports and medicine. In the present work we performed a forward dynamic analysis of both the gait cycle and squat. For that, we used a 2D multibody system implemented in MATLAB and data acquired in the Biomechanics of Motion Laboratory at Instituto Superior Técnico. The model was employed to analyze the ground reaction forces, joint moments and joint powers in the gait cycle and squatting motion of a healthy female at the level of the lower limb joints (hip, knee, and ankle) and muscles. For the gait, a hip dominant gait was observed. For the squat, given the deviations in the experimental procedure, the results led to suggestions for protocol improvement, since they differed from those in the literature.*

1. Introduction

The dynamic analysis of a multibody system regards the study of the motion of the system, as a result of the forces involved in the motion and then inertial characteristics of the system. This analysis can be achieved through multibody dynamic formulations, based in cartesian, natural or joint coordinates or Kane's formalism [1], however, similarly to the kinematics analysis, cartesian coordinates will be used.

For the present work, a forward dynamic analysis was performed for the gait cycle and the squat, in order to obtain the joint reaction forces and moments, and analyze the forces involved in both movements. For that purpose, we resorted to MATLAB taking into consideration the previous kinematic implementations and results [2]. Hence, in the report only new steps or results will be presented, as well as relevant commentaries to link both analyses.

1.1. Motivation

Body movements require a highly coordinated mechanical interaction between bones, muscles, ligaments and joints, and play a major role in our day-to-day life. For that, both kinematic and dynamic analysis are an important tool in a variety of fields, having applications such as therapy and diagnosis, optimization of athletic performances, or even the design of biomedical devices, such as prosthesis. Indeed, the kinetic analysis assumes particular relevance in this context since one can also retrieve the body positions based only on the force's acquisition.

Since the gait cycle is one of the most common human movements, its analysis can be of high interest and can help accessing and treating difficulties in an individual's walking. On the other hand, the proper performance of the squat benefits not only athletes and their performance, but a grand majority of the population, since it is considered one of the best exercises to improve quality of life, since it is able to recruit several muscle groups [4].

2. Methodology

A forward dynamic analysis was performed in order to analyze both motions described above, using both kinematic and kinetic data acquired in the lab and the kinematic analysis program developed previously.

2.1. Equations of motion

The equations of motion can be obtained through the Principle of Virtual Power, which states that the virtual power for a multibody system is zero:

$$P^* = \dot{q}^{*T} f \iff P^* = \dot{q}^{*T}(M\ddot{q} - g) = 0 \tag{1}$$

Where $\dot{q}$ represents the vector of virtual velocities, $M\ddot{q}$ the inertial forces (with M being the matrix of overall mass of the system and $\ddot{q}$ the vector of generalized accelerations) and g the external forces. It is important to note that the force vector f does not contain the internal forces associated with the kinematic constraints (joint reaction forces), however they still need to be introduced in the equations of motion. With that purpose, the Lagrange multipliers method is used, and the internal forces are given by $g_{int} = -\Phi_q^T \lambda$, with λ the vector of the Lagrange multipliers. Since the virtual power of the internal forces is also zero, equation 1 can be written as [3]:

$$P^* = \dot{q}^{*T}\left(M\ddot{q} + \Phi_q^T \lambda - g\right) = 0 \iff M\ddot{q} + \Phi_q^T \lambda = g \tag{2}$$

To solve this system, an extra set of equations is necessary, the acceleration kinematic constraint equations, which are given by $\Phi_q \ddot{q} = \gamma$. Bearing all this in mind, the complete set of equations necessary to obtain the solution of the dynamic analysis is given by [1][3]:

$$\begin{cases} M\ddot{q} + \Phi_q^T \lambda = g \\ \Phi_q \ddot{q} = \gamma \end{cases} \Rightarrow \begin{bmatrix} M & \Phi_q^T \\ \Phi_q & 0 \end{bmatrix} \begin{Bmatrix} \ddot{q} \\ \lambda \end{Bmatrix} = \begin{Bmatrix} g \\ \gamma \end{Bmatrix} \tag{3}$$

The solution of the system can be achieved by solving the initial value problem in equation 4. We start by defining a set of initial conditions, q and $\dot{q}$, and proceed to solve equation 3 for the unknown accelerations, for the current time step. Having this, we can then obtain the velocities and accelerations for the next time step.

$$\begin{cases} M\ddot{q} + \Phi_q^T \lambda = g \\ \Phi(q, t) = 0 \end{cases} \tag{4}$$

It is important to note that only the acceleration constraint equations will be explicitly used in the process, which leads to the propagation of numerical errors. To control this, we use Baumgart stabilization. Finally, equation 3 can be rewritten [1][3]:

$$\begin{bmatrix} M & \Phi_q^T \\ \Phi_q & 0 \end{bmatrix} \begin{Bmatrix} \ddot{q} \\ \lambda \end{Bmatrix} = \begin{Bmatrix} g \\ \gamma - 2\alpha\left(\Phi_q \dot{q} - v\right) - \beta^2 \Phi \end{Bmatrix} \tag{5}$$

Where α and β are positive constants (both 15 in our program), providing the necessary stability of the solution. Further details on the equations and methods used can be found in Appendix B.

2.2. Implementation

The multibody system implemented for the dynamic analysis was the same as the one considered in the kinematic analysis [2], i.e. the same bodies, joints, and drivers were considered. However, for the dynamic analysis one should also consider the kinetic data collected at the laboratory. An overall picture of the implementation of our model

can be seen in Figure 1. Since the 2D model considered was the same as the one elaborated for the first part of this project [2]**,** only some additional steps needed to be implemented, which are marked in figure in bold.

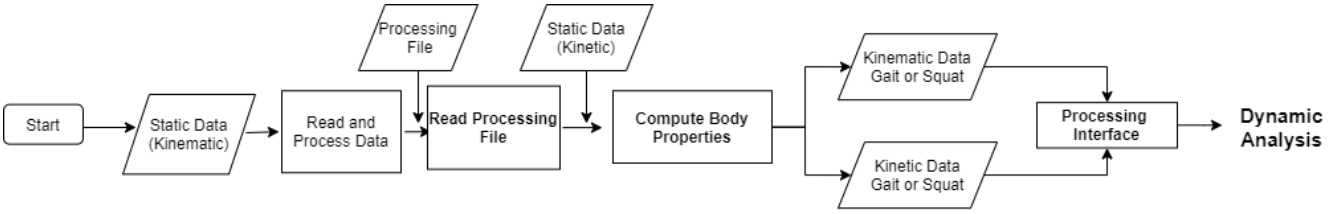

Fig. 1: Flowchart of the implemented dynamic analysis program.

For the dynamic analysis, not only are we interested in the coordinates obtained in the laboratory, but also in the kinetic data, i.e. the centers of pressure (**COP**) and the ground reaction forces (**GRF**) collected from the three different force plates. However, before being able to use the raw data registered at the laboratory, a pre-processing step also had to be done to both coordinates of the **COP** and **GRF** (corresponding to the sagittal plane). The pre-processing step of the kinematic data has already been explored at further extent in the first part of this project, being its basis a residual analysis of the data for each coordinate with subsequent filtering with the obtained cut-off frequencies (which can be found in Figure C.1 in Appendix C).

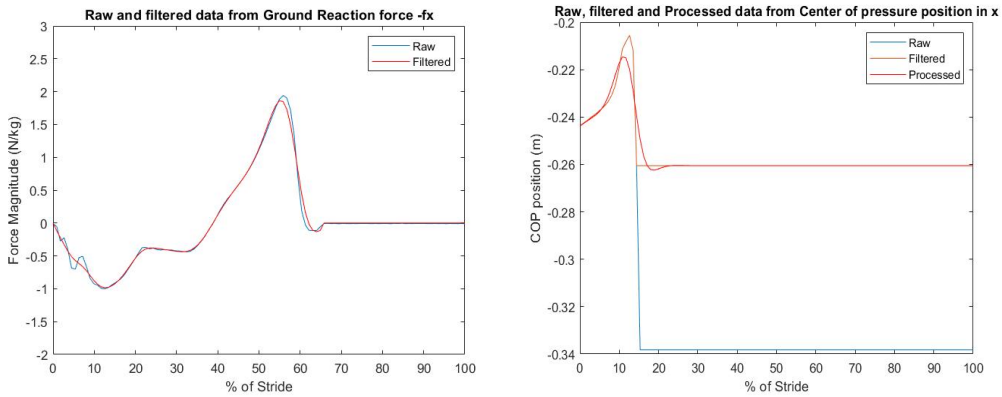

Fig. 2: a) GRF: comparison between Raw data (blue) and filtered Forces (red), considering its x-component in the second pressure plate. b) COP: comparison between Raw (blue), Filtered(red) and Processed (black) COPs, considering its x-component in the first pressure plate.

As a first processing step, all forces collected in the laboratory which were smaller than 5 Newtons were considered as artefacts and thus considered to be null. Then, both the resulting processed GFR and COP data were filtered using a low-pass Butterworth filter with a cut-off frequency of 10 Hz. Higher cut-off frequencies were tested for the GRF data (20 Hz, for example). However, these were not sufficient to smooth the data obtained in the laboratory. This observation may already anticipate some irregularities of the results obtained in our dynamic analysis when compared to literature. Figure 2 illustrates the differences between the Raw and Filtered data for both data types. Finally, an additional processing step was considered for the COP: all the discontinuities found in the filtered data, which were caused because the foot was no longer in contact with the pressure plate were removed. For that, the coordinates were prolonged to the last known position before the discontinuity. The resultant Processed data can also be seen in Figure 2b. Since different time steps than the ones obtained from the laboratory might be needed for the dynamic analysis, cubic splines were also applied to the COP and GRF data after processing.

Throughout our program, a set of global variables is defined into structs (shown in Table D.1, in Appendix D). To perform a dynamic analysis, additional anthropometric data and other known inputs had to be added to the

previously developed Processing File for the kinematic analysis. In addition to the positions of the center of mass of each body, the normalized mass and radius of gyration were also necessary, which were withdrawn from Table A.1, Appendix A. Much like before, the computation of the average length of each body was done using the data for the static position, from which the kinetic data, more specifically the GRF data, was now used to compute the total body mass of our model. The anthropometric data now allowed us to obtain the mass and moment of inertia of each rigid body, which is implemented in the function *Compute Body Properties.*

Once we have completed the definition of our global variables *Body*, *Jnt* and *FPlate*, we can then proceed to the dynamic analysis. For this, the flowchart followed can be seen in Figure D.1, Appendix D. After correcting the initial conditions, to make sure that the kinematic constraints are fulfilled, the system of equations described in B is constructed to obtain the different accelerations (with regards to each coordinate) of each body and these are subsequently integrated in time along with the velocities from the initial conditions. This process is repeated for every time step desired, using the velocities calculated in the previous iteration, which allows for the computation of the coordinates of the positions and velocities of each body for the time length of the movement.

The equations of motion are then calculated once again for each time instant, using the now obtained kinematic data, to obtain the Lagrange multipliers associated with the kinematic constraint, so as to calculate the internal forces and moments of each joint.

3. Results and Discussion

This section focuses on displaying and critically assessing the results that have been obtained, in the kinetic analysis of both the gait cycle and the squat, regarding ground reaction forces, joint moments/torque and joint powers. When relevant, these were also correlated with muscle activation patterns, which were obtained via EMG. Despite having already analyzed the EMG data in our previous work [2], we believe that the current setting allows for a more comprehensive and meaningful analysis of the correlation between muscle activity and the movement.

3.1. Gait cycle

We have previously observed the gait cycle from a kinematic point of view [2], having concluded that it seemed normal for a healthy individual. The cadence was 108 steps/min, which corresponds to a natural cadence walk, and the different phases of the gait cycle were easily identifiable.
However, further scientifically and clinically relevant analyses can be conducted in order to determine the forces at play during the gait cycle, which can be posteriorly reviewed so as to best determine the basics of the gait cycle, the physical condition of the individual and, if necessary, the best route of treatment for an eventual pathology. This section will therefore explore ground reaction forces, joint moments and joint powers associated with the gait cycle.

3.1.1. Ground reaction forces

Newton's Third Law of Motion states that "For every action, there is an equal and opposite reaction" [5]. The ground reaction forces, in a way, can be seen as exactly that: the equal and opposite reaction to the force inflicted upon the ground (or in this case upon the detection mechanism, i.e. the different force plates) by the subject. These can be divided into different components, x and z, which represent the horizontal and vertical components (respectively) of the force in the plane of motion.

As can be seen in Figure 3, the horizontal forces are initially negative, as the ground reacts to the forward motion of the body, which corresponds to a decrease in the body's velocity. As the body is gaining momentum by pushing

the ground in the opposite direction of the movement, the horizontal forces become positive, since the ground reacts to that push by pushing the foot away in the direction of the movement. The horizontal reaction forces, despite being always greater than zero (since the ground is always pushing the body upwards), have 2 distinct peaks, which occur when the full weight of the body is initially set on the foot contacting the ground and when the body pushes the ground in order to lift the leg.

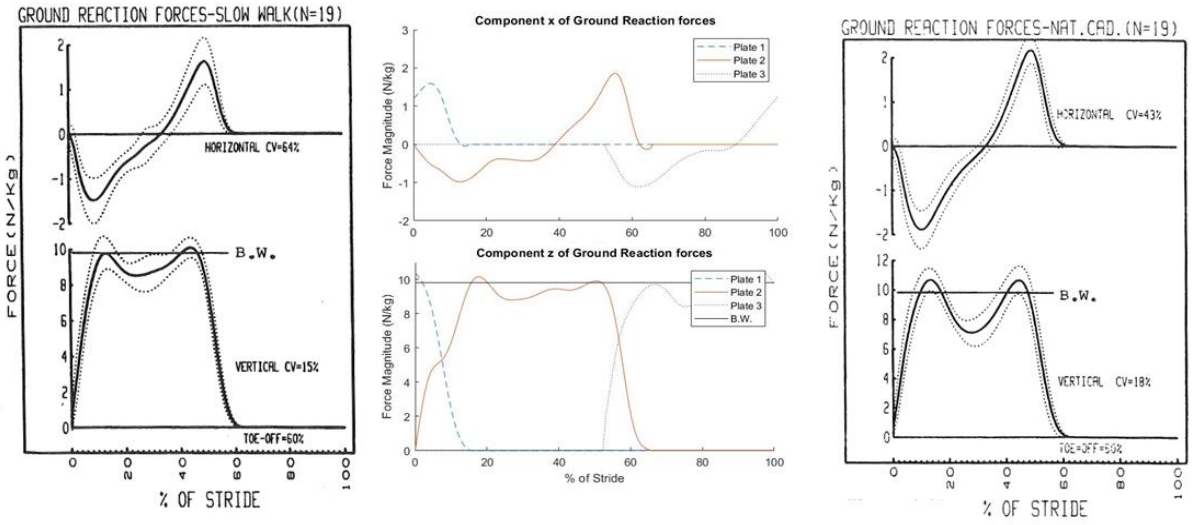

Figure 3 - Ground reaction forces in each force plate by completed percentage of stride (N/m). Left panel: literature results for slow walk according to Winter *et al*.; Middle panel: results obtained in our experiment; Right panel: literature results for natural cadence according to Winter *et al* [6].

As seen in our previous work, our subject's cadence was 108 steps per minute [2], which corresponds to a natural walking cadence [8]. However, it is evident that, even adjusting the scales, there are three major discrepancies between our data and those available in the literature, namely one hump in the graph for the horizontal reaction forces (at roughly 22-36% of the stride) and a shoulder and a hump in the graph for the vertical reaction forces (at roughly 5-10% and 37-45% of the stride, respectively). We believe that these are due to our subject's lack of experience in performing these studies, and to the fact that these measures are unique, not having been reproduced enough times. To develop a bit further, the inexperience of our subject may have caused some indecision in their stride because they were told to try to place their feet on the force plates, causing a conscious override of an otherwise unconscious movement that may have deteriorated the data, causing an involuntary shift between cadences during the stride. This feature was not particularly evident earlier, as the kinematic analysis of the motion provided more simplistic data in what concerns the cadence of the gait. The deterioration of these results, as previously stated, could have been dampened by considering multiple trials, and taking the average. Unfortunately, since this analysis is performed *a posteriori*, that scenario was impossible. These findings are further verified by the strong emphasis on the heel strike when compared to the literature [7], which can be seen in the center of pressure (COP) as depicted in Appendix E. Therefore, our walking profile seems to have more correlation with the slow cadence walking profile, instead of the expected natural cadence, at least in what concerns the ground reaction forces. From here on after, both profiles will be considered for comparisons with literature data, in order to try and better comprehend our results.

3.1.2. Joint moments

The joint moments of the body represent the entire forces which act upon a joint. These can be a result of muscle, ligament or hamstring activity, and take into account friction (although the latter is often negligible in the cases where the amplitude of the joints does not reach its extrema, which is what happens in our case). Figure 4 depicts

the joint moments of the right limb joints across stride completion, as well as the support moment, while comparing them to literature data. The support moment is defined by Winter as $M_s = M_a + M_k + M_h$[6], where $M_a$is the joint moment around the ankle, M_k is the joint moment of the knee and M_h represents the joint moment of the hip.

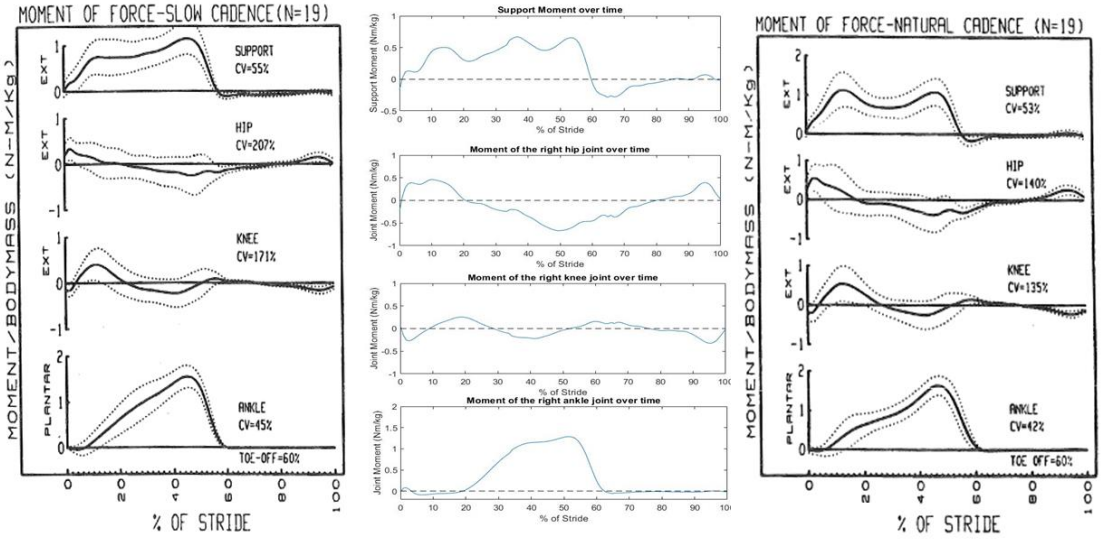

Figure 4 - Joint moments for the right limb (Nm/kg). Left panel - literature for slow cadence walk [6]; Middle panel - experimental results; Right panel - literature data for natural cadence walk[6].

With an attentive look at Figure 4, one can see that the data obtained in our experiment lie well within the variability range described in the literature for individual moments for both slow and natural cadence walks, especially for the individual joint moments, but for the support moment as well. The biggest discrepancy that can be found relates to an unexpected peak in the support moment, which is caused by a small increase in the hip joint moment and an abnormally early increase in the ankle moment. However, comparing Figures 3 and 4, one can easily note that this moment coincides with the moment when the horizontal ground reaction force displays an abnormal behavior, and therefore both abnormalities seem to originate in the aforementioned restrictions of the experimental setting, i.e., the conscious override of an acquired habit. Focusing our attention on the hip joint moment, we can also see that the gait of this specific individual seems to be particularly driven by the hip, since the experimental values for the hip joint moments cover mostly the entire range of the natural variance.

3.1.3. Joint power

Joint power can be seen as a dynamic measure of the energy stored in the muscles which act upon each joint, as they move eccentrically or concentrically, and is formally calculated with $P_j = M_j \times w_j$, where M_j is the joint's moment and w_j is the joint's angular velocity. A negative value of P_j implies energy absorption by the muscle (eccentric contraction), while a positive value of $P_j$means that the muscle is generating energy to be used in the movement (concentric contraction).

As can be seen in Figure 5, the recruitment of right limb muscles varies greatly throughout the gait cycle, even for the same individual. Initially, as the right leg swing ends and the weight gradually shifts from the left foot to the right foot, the hip and knee joints, which were previously exerting concentric contraction, switch to eccentric contraction and a neutral state, respectively. Afterwards, as the subject exerts force in order to lift the foot off the ground, there is a great increase in ankle power, followed by a simultaneous energy absorption by the knee and energy generation by the hip, as the right limb is lifted into the air, whereafter all joints return to state of relative inaction. Lastly, the hip power increases as knee power decreases, preparing the following heel strike of the right

limb. Note that here the confounding effect of consciously walking appears to be much less present, only being noticeable in the quick variations that can be seen in the graphs for hip and ankle power. This leads us to believe that muscle contraction is not a direct representation of how the movement is performed, which is quite senseful: there are many more variables at play, such as the size of the individual and the way they shift their weight throughout the movement, which ultimately contribute to the final movement. The data for joint power further hints that this particular gait cycle was performed with an extraordinary emphasis on the hip, since the values for the H3 peak of concentric hip contraction are abnormally high when compared with the literature data for either cadence. This might be explained by the fact that this particular individual is a recreational dancer and might thus have acquired some unusual habits in what regards muscle contraction of the lower limbs.
The Electromyography (EMG) data for the gait cycle can be found in Appendix F and further confirm these results, since the activation of the muscles around each joint coincides with the trend of the joint power curves.

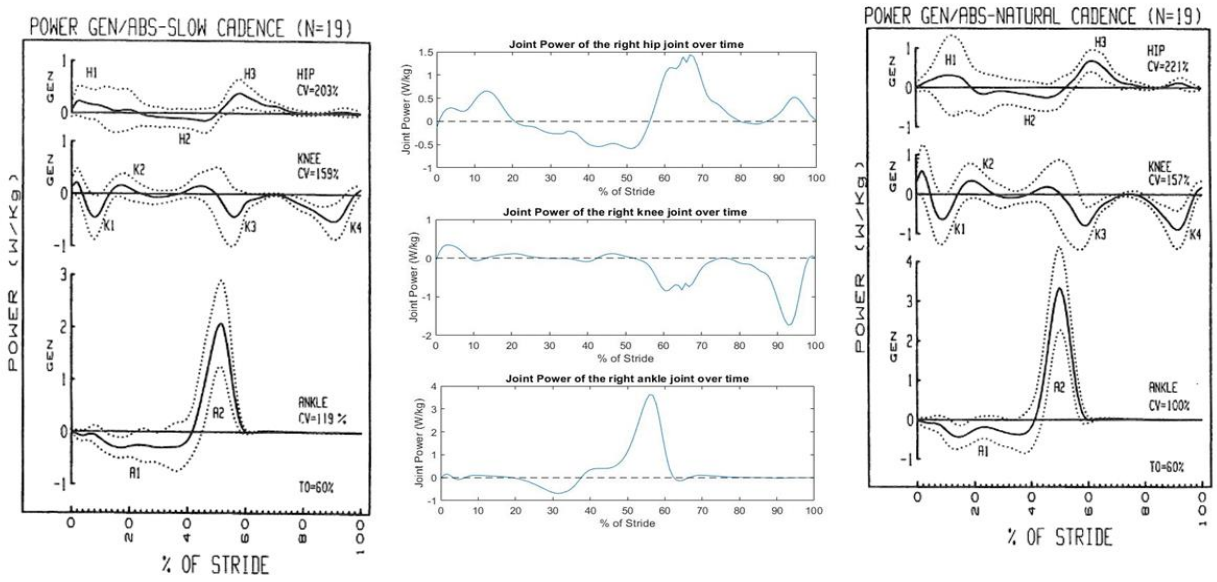

Figure 5 - Joint power for the right limb (W/kg). Left panel - literature for slow cadence walk [6]; Middle panel - experimental results; Right panel - literature data for natural cadence walk [6].

3.2. Squat

As for the gait cycle, the kinematic analysis of the squat highly benefits from being complemented with the analysis of the forces that are relevant to the movement. In our previous study, we reported a normal squat, since the slight differences between our data and the literature could be attributed to inherent subject variability. Focus was particularly laid on the flexion angles of the joints throughout time, since the squat is mostly a one-dimensional movement.
In the following section we will analyze the ground reaction forces, joint moments and joint powers of the lower right limb. Since the squat is a symmetrical movement along the sagittal plane, the results should be equally valid for the left limb.

3.2.1. Ground reaction forces and COP

In this case, the ground reaction forces themselves (depicted in Figure 6) are not particularly interesting. Horizontally, we see minimal (yet not null) force in a semi-erratic pattern, which is to be expected, since the squat is a movement without horizontal progression. As for the vertical reaction forces, we can see a semi-constant threshold for all three squat trials, which corresponds to the acceleration phase of the squat. The ground reaction

force then suddenly increases, as the squat enters its deceleration phase, where the subject pushes against the ground in order to rise back up to the standing position, re-entering the threshold phase.
It is already evident, from the comparison of the curves corresponding to the three different trials, that this movement has great variability even within the same subject, which will sadly prove to be a prominent source of data deterioration.

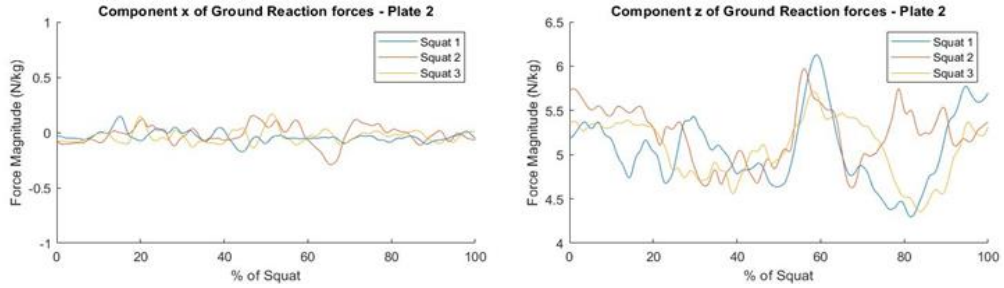

Figure 6 - Right limb's ground reaction forces throughout stages of the squat for three different squat trials (N/kg). Left - horizontal reaction forces; Right - Vertical reaction forces.

A more interesting analysis that can be performed relates to the position of the center of pressure.

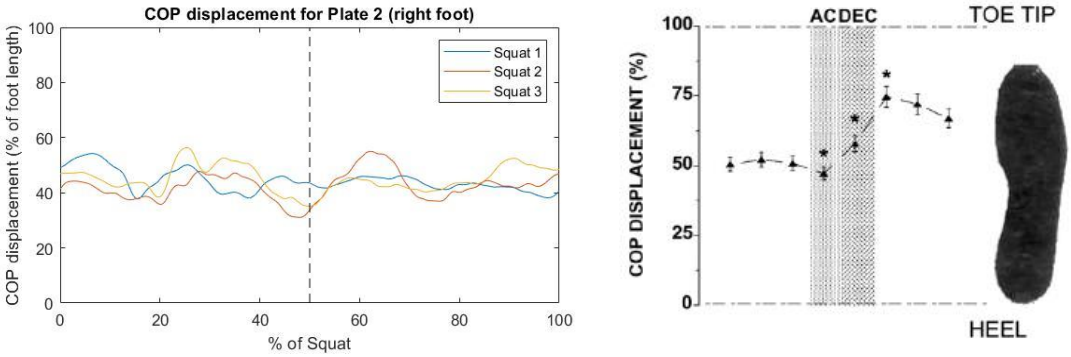

Figure 7 - COP displacement as a percentage of the length of the foot. Left - experimental data; Right - literature data for half squat (70º) with fixed upper body[9]. AC and DEC stand for acceleration phase and deceleration phase, respectively.

As can be seen in Figure 7, the COP, defined as the moment in the y coordinate (perpendicular to the plane of motion) divided by vertical force, shows high variations throughout time. Just as for the gait, this measure is a representation of where in the foot the pressure applied by the vertical forces and the movement of the body is the highest. What is interesting to note is that, while the literature presents a defined line for the displacement of the COP throughout the squat [9], our results seem to have a semi-random distribution around the center of the foot. Indeed, this is further represented by the fact that there does not seem to be a recognizable pattern among all 3 squat trials. This hints at the fact that our movement might not have been performed as well as we initially thought, although it is important to note that the reference results are obtained by averaging results from different participants, which were told to squat as fast as possible to an angle of 70º while maintaining their torso in an erect position.
So, although we would expect a posterior displacement of the COP during the acceleration phase (until roughly 50% of the squat has been completed [2]), followed by an accentuated anterior displacement of the COP [8], what we actually observe is that the COP is always roughly around the 50% mark, most likely because none of the aforementioned constraints (especially the position of the torso, which might have been the most important one) were not applied in our experiment. Logically, this hypothesis will have to be verified by our further results.

3.2.2. Joint Moments

Figure 8 depicts the joint moments obtained for the ankle and the knee throughout the various repetitions of the squat, as well as literature results for those very moments. Once again, it is easily noticeable that our results do not coincide with those obtained in the more controlled experiments performed by Dionisio and colleagues [9], which, beside the aforementioned factors, might have to do with the speed of the squat - ours was performed at a much slower pace, since the subjects of the reference study were instructed to squat as fast as possible. Even within themselves, our results seem to show great variability, especially for the ankle. While a pattern is still somewhat recognizable for the moment of the knee, the moment of the ankle seems to have a semi-random distribution around the value of -0.3Nm/kg. Just as we have previously seen with the COP, these results most likely originate from the lack of restrictions imposed to our subject, and are almost certainly a consequence of the unconscious attempt to minimize the effort required for this movement, by keeping the center of pressure around the middle of the foot.

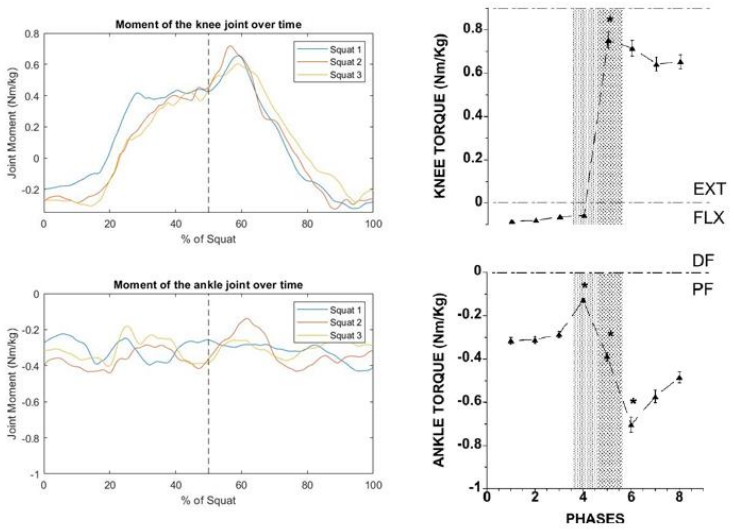

Figure 8 - Joint moments for the ankle and the knee over the progression of the squat (Nm/kg). Left - experimental data; Right - data retrieved by Dionisio *et al* [9].

The muscle activation patterns that can be seen in Appendix F further solidify these results: comparing our results with the aforementioned reference, we see that the activity of the rectus femoris is diminished and the activity of the gastrocnemius is heavily reduced in our setting. On the other hand, the activities of the biceps femoris and tibialis anterior are increased when compared to reference data. This is a pattern which is typical of a forward-leaning motion, where the trunk is not erect and the knees have the freedom to advance further than the toes.

Another restriction that could have been applied regards exactly this previous point. Fry *et al.* [10] found that restricting the advance of the knee has a significant impact on the moments of the hip and knee joints, as well as in muscle activation. Indeed, placing a wooden board immediately in front of both feet, therefore inhibiting excessive advances of the knee, greatly increased hip torque while moderately reducing knee torque. Although those squats were performed while holding a barbell, and might therefore not be directly comparable, the results obtained by Fry *et al*. certainly show that even the smallest variations in performing a movement can have a great impact on the joints and muscles that are responsible for said movement. This observation has two direct consequences: on one hand, it further shows us that our data has too many uncontrolled variables and should be refined for further studies. One the other hand, it reinforces the need for thorough biomechanical studies and proper support of patients with lower limb impairments, effectively adding value, but also responsibility, to the work of physiotherapists.

3.2.3. Joint power

Figure 10 illustrates the joint power that was measured in each joint throughout the completion of the squat. Although these values seem abnormally low, and the literature was lacking in providing data for a scenario similar to ours, we can still observe a pattern in the three trials performed. This is especially evident in the case of the hip

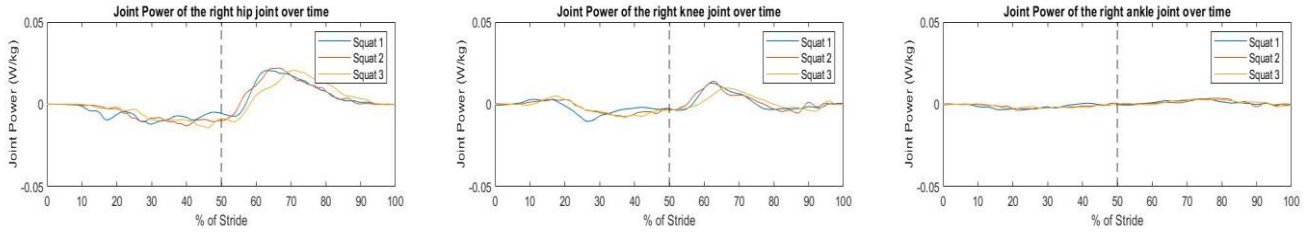

Figure 10 - Joint power for hip, knee and ankle during the squat. All 3 trials are represented, each with its respective color.

and the knee, where there seems to be a reduction in joint power during the acceleration phase, as the body descends, absorbing energy, which is followed by an increase in power during the deceleration phase, as the muscles are recruited to bring the body to an upright position.

However, as previously stated, the reliability of these data is very low, since the values presented seem too small, even without an accurate frame of reference. Experiments performed in different settings, often with weights, always achieved much higher joint power values [11],[12] (even after normalization and accounting for the fact that weights were involved), and thus further, more controlled experiments should be performed to confirm the validity of our data, preferably including some of the restraints that have been mentioned above.

4. Conclusions

In this project, we analyzed the kinetics of gait and squat movement of a healthy subject, using a MATLAB implementation. A general conclusion that can be drawn is that kinematic studies should always be complemented with kinetic studies, or even replaced by them, since it is possible to retrieve the position of the body from its forces, but not the forces from the position. Kinetics helps us to understand how the movement is really being performed, based on the distribution of forces and torques. In our particular case, we observed that the gait cycle was predominantly set by the hip and, despite its apparent natural cadence (108 steps/min), the experimental inexperience of the subject led to hesitation in the stride, which conferred some of the characteristics of a slow cadence gait to the otherwise natural gait of the subject. Regarding the squat, we found high discrepancies between our results and the literature, which we believe come from the lack of restrictions imposed upon the subject during the experiment. The fact that our results are not consistent among themselves, as all 3 squat trials appear to follow different patterns, further validates this conclusion.

5. Other Remarks

As mentioned before, in this work, it has become evident that biomechanical motion is quite variable, not only between individuals, but within the same individual, if the appropriate restrictions are not applied. Thus, it becomes even more critical to be able to analyse patterns instead of values. In the setting of physiotherapy, it is crucial to understand that each individual is different from the others and progresses in its own way. With this much variability, one can definitely see the value of attentive and close support of the patient by the physiotherapist and the importance of the communication of the results and improvements of the patient to the doctor.

Additionally, in our previous work, we proposed an alternative method for kinematic analysis, which was based on machine learning - self-organising maps (SOMs). However, this method is only adequate for a kinematic analysis, since its data acquisition is based on visual cues only. Thus, an analysis of the internal forces with SOMs, which might be crucial to understand the movement in its full capacity (as was shown in this work), is impossible.

References

[1] Ambrósio, J. A. C., & Kecskeméthy, A. (2007). Multibody dynamics of biomechanical models for human motion via optimization. Computational Methods in Applied Sciences, 4, 245–272.

[2] Santos, A., Marques, D., Baltazar, F., and Martins,R. (2020). "Kinematic Analysis of Human Gait Cycle and Squat", Instituto Superior Técnico, Lisbon.

[3] Ambrósio, J. "Kinematics of multibody systems." Week 08, Lecture 22, 2020.

[4] Schoenfeld, B. J. (2010, December). Squatting kinematics and kinetics and their application to exercise performance. *Journal of Strength and Conditioning Research*, Vol. 24, pp. 3497–3506. https://doi.org/10.1519/JSC.0b013e3181bac2d7

[5] Newton's laws of motion - Wikipedia (accessed on 29/12/2020)

[6] Winter, D. (1987). The biomechanics and motor control of human gait. University of Waterloo Press.

[7] Li, B., Xiang, Q. & Zhang, X. The center of pressure progression characterizes the dynamic function of high-arched feet during walking. *J Leather Sci Eng* 2

[8] Bouchard, D.R. , Slaght, J., Sénéchal, M., Hrubeniuk, T. J., Mayo, A. Walking cadence to exercise at moderate intensity for adults: a systematic review. Hindawi Press, 2017

[9] Dionisio, V. C., Almeida, G. L., Duarte, M., & Hirata, R. P. (2008). Kinematic, kinetic and EMG patterns during downward squatting. Journal of Electromyography and Kinesiology, 18(1), 134–143. https://doi.org/10.1016/j.jelekin.2006.07.010

[10] Fry AC, Smith JC, Schilling BK. Effect of knee position on hip and knee torques during the barbell squat. J Strength Cond Res. 2003 Nov;17(4):629-33. doi: 10.1519/1533-4287(2003)017<0629:eokpoh>2.0.co;2. PMID: 14636100., 1 (2020).. https://doi.org/10.1186/s42825-019-0016-6

[11] Hwang, S., Kim, Y. & Kim, Y. Lower extremity joint kinetics and lumbar curvature during squat and stoop lifting. *BMC Musculoskelet Disord* 10, 15 (2009). https://doi.org/10.1186/1471-2474-10-15

[12]Jandacka D, Uchytil J, Farana R, Zahradnik D, Hamill J. Lower extremity power during the squat jump with various barbell loads. Sports Biomech. 2014 Mar;13(1):75-86. doi: 10.1080/14763141.2013.872287. PMID: 24968512.

Appendix

Appendix A. Anthropometric data

Table A.1: Mass, center of mass location and radius of gyration. Retrieved from Winter, D. A. (2009). Biomechanics and Motor Control of Human Movement: Fourth Edition. In *Biomechanics and Motor Control of Human Movement: Fourth Edition*.

Segment	Definition	Segment Weight/Total Body Weight	Center of Mass/ Segment Length		Radius of Gyration/ Segment Length		
			Proximal	Distal	C of G	Proximal	Distal
Hand	Wrist axis/knuckle II middle finger	0.006 M	0.506	0.494 P	0.297	0.587	0.577 M
Forearm	Elbow axis/ulnar styloid	0.016 M	0.430	0.570 P	0.303	0.526	0.647 M
Upper arm	Glenohumeral axis/elbow axis	0.028 M	0.436	0.564 P	0.322	0.542	0.645 M
Forearm and hand	Elbow axis/ulnar styloid	0.022 M	0.682	0.318 P	0.468	0.827	0.565 P
Total arm	Glenohumeral joint/ulnar styloid	0.050 M	0.530	0.470 P	0.368	0.645	0.596 P
Foot	Lateral malleolus/head metatarsal II	0.0145 M	0.50	0.50 P	0.475	0.690	0.690 P
Leg	Femoral condyles/medial malleolus	0.0465 M	0.433	0.567 P	0.302	0.528	0.643 M
Thigh	Greater trochanter/femoral condyles	0.100 M	0.433	0.567 P	0.323	0.540	0.653 M
Foot and leg	Femoral condyles/medial malleolus	0.061 M	0.606	0.394 P	0.416	0.735	0.572 P
Total leg	Greater trochanter/medial malleolus	0.161 M	0.447	0.553 P	0.326	0.560	0.650 P
Head and neck	C7–T1 and 1st rib/ear canal	0.081 M	1.000	— PC	0.495	0.116	— PC
Shoulder mass	Sternoclavicular joint/glenohumeral axis	—	0.712	0.288	—	—	—
Thorax	C7–T1/T12–L1 and diaphragm*	0.216 PC	0.82	0.18	—	—	—
Abdomen	T12–L1/L4–L5*	0.139 LC	0.44	0.56	—	—	—
Pelvis	L4–L5/greater trochanter*	0.142 LC	0.105	0.895	—	—	—
Thorax and abdomen	C7–T1/L4–L5*	0.355 LC	0.63	0.37	—	—	—
Abdomen and pelvis	T12–L1/greater trochanter*	0.281 PC	0.27	0.73	—	—	—
Trunk	Greater trochanter/glenohumeral joint*	0.497 M	0.50	0.50	—	—	—
Trunk head neck	Greater trochanter/glenohumeral joint*	0.578 MC	0.66	0.34 P	0.503	0.830	0.607 M
Head, arms, and trunk (HAT)	Greater trochanter/glenohumeral joint*	0.678 MC	0.626	0.374 PC	0.496	0.798	0.621 PC
HAT	Greater trochanter/mid rib	0.678	1.142	—	0.903	1.456	—

Appendix B. Details on the equations used

B1. Baumgart stabilization

The system given by equation 3, section 2, is an open-loop system, leading to error propagation. To correct this, we apply the Baumgart stabilization method, by substituting the unstable equation by an equation of the form $\ddot{y} + 2\alpha\dot{y} + \beta = 0$. Since only the acceleration constraint equations will be explicitly used in the process, it is the one requiring stabilization:

$$\ddot{\Phi}(q,t) = 0 \rightarrow \ddot{\Phi} + 2\alpha\dot{\Phi} + \beta^2\Phi = 0 \rightarrow \left(\Phi_q\ddot{q} - v\right) + 2\alpha\left(\Phi_q\dot{q} - v\right) + \beta^2\Phi = 0$$

$$\Rightarrow \Phi_q\ddot{q} = \gamma - 2\alpha\left(\Phi_q\dot{q} - v\right) - \beta^2\Phi \tag{B.1}$$

B2. Mass Matrix

The mass matrix in equation 5, section 2, is symmetric and diagonal, with each entrance being the individual mass matrices of each body i, M_i, which is calculated using the anthropometric data in Appendix A.

$$M_i = \begin{bmatrix} m_i & 0 & 0 \\ 0 & m_i & 0 \\ 0 & 0 & J_I \end{bmatrix} \tag{B.2}$$

With m_i and J_i being each body's mass and moment of inertia, respectively.

B3. Forces and Moments

The vector of external forces, g, is a generalized vector that includes the forces applied in each of the rigid bodies, i.e., the gravity forces and the contact forces, hence for a system with n bodies, $g = [g_1,\ g_2, \dots, g_n]^T$. For each body i we have a vector g_i, which entrances are the force f and the moment n applied on it.

$$g_i = \begin{Bmatrix} f_x \\ f_y \\ n + n_{transport} \end{Bmatrix}_i = g_{i,gravity} + g_{i,contact} \tag{B.3}$$

The term $n_{transport}$ corresponds to the resultant moment from transferring the applied force from the point of its application, to the center of mass of the body,

$$n_{transport} = s_i^P \times f_i = s_x^P f_y - s_y^P f_x \tag{B.4}$$

Appendix C. Cut-off frequencies

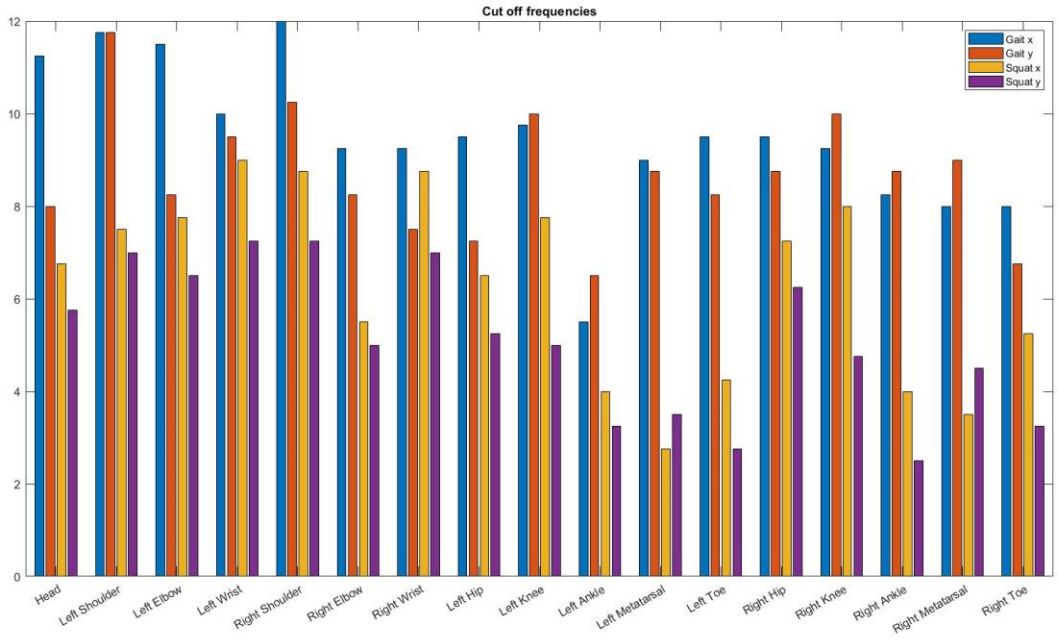

Fig. C.2: Cut-off frequencies used to filter the position data of each body, for both movements.

Appendix D. Details on the implementation

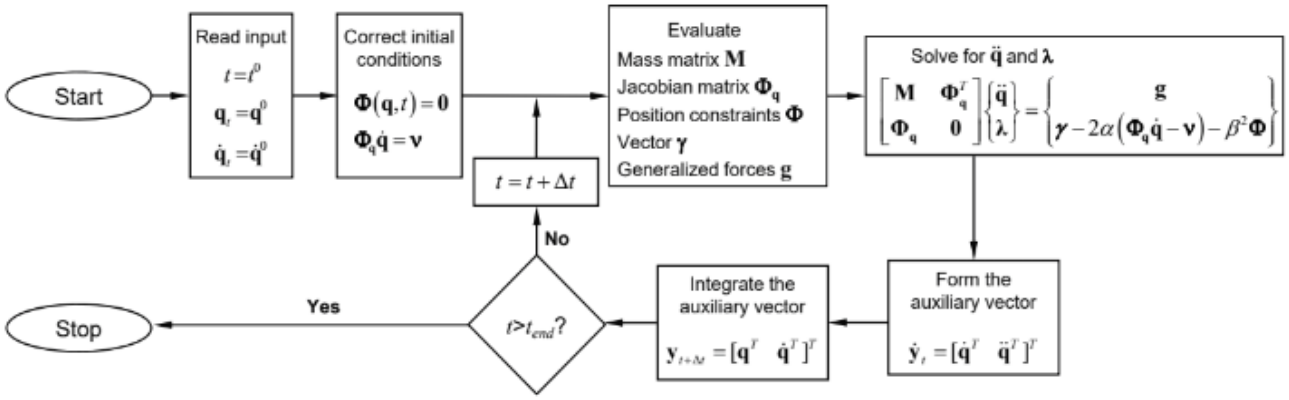

Fig. D.1: Flowchart for the forward dynamic analysis. (por esquema prof aula 22, semana 8, slide 21)

D1. Structs' Organization

Table D.1- Information contained on each struct. Global variables: Data/ Static Data, Body, Jnt, FPlate and Output. Further explanation for a better code understanding is presented in directly commented on the MATLAB script.

Data/Static Data	**Body**	**Jnt**	**FPlate**
• Frequency • Coordinates	• Number • PtsAdj • COM • Pi • Pj • Length • theta • Eta • r • csi • A • B	• NRevolute • NGround • NDriver • Revolute - i - j - spPi - spPj • Driver - type - i -ctype - j -Data - q - qd - qdd	• Number • i • j • Data • mx • mz • copx • copz
Output			
• Time	• Body - r - theta - thetad - rdd - thetadd - COM	• NRevolute	• Revolute - Fx1 - Fz1 -M1 - thetad

Appendix E. Path of Center of Pressure on the right foot

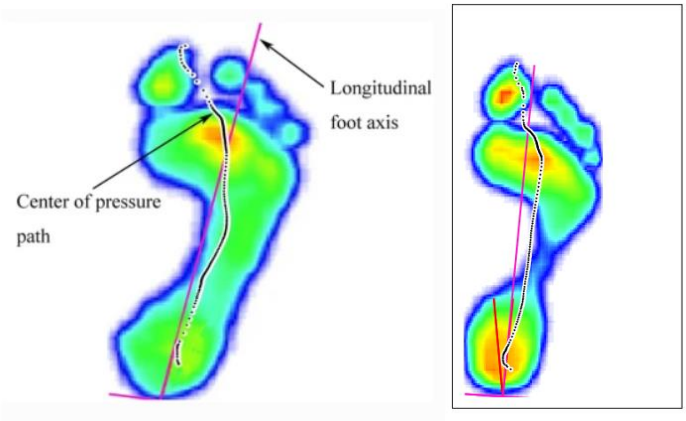

Fig. E.1: Left - literature data; Right - experimental data. There is a clear difference in the progression of the COP, as well as in the values of pressure detected in the heel, which can explain some of the slightly abnormal behavior discussed in section 3.1. (red - longitudinal foot axis; black - path of COP)

Appendix F. EMG data for the gait cycle

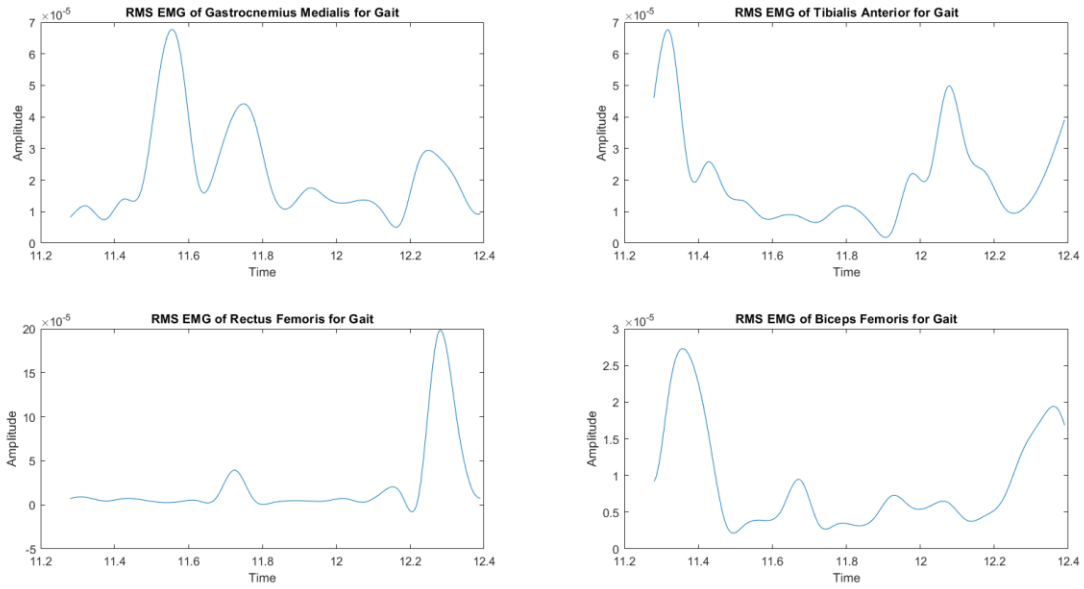

Fig. F.1: RMS EMG data for different muscles during one gait cycle. Top left - Gastrocnemius Medialis; Top right - Tibialis Anterior; Bottom Left - Rectus Femoris; Bottom Right - Biceps Femoris.

Appendix G. EMG data for the squat

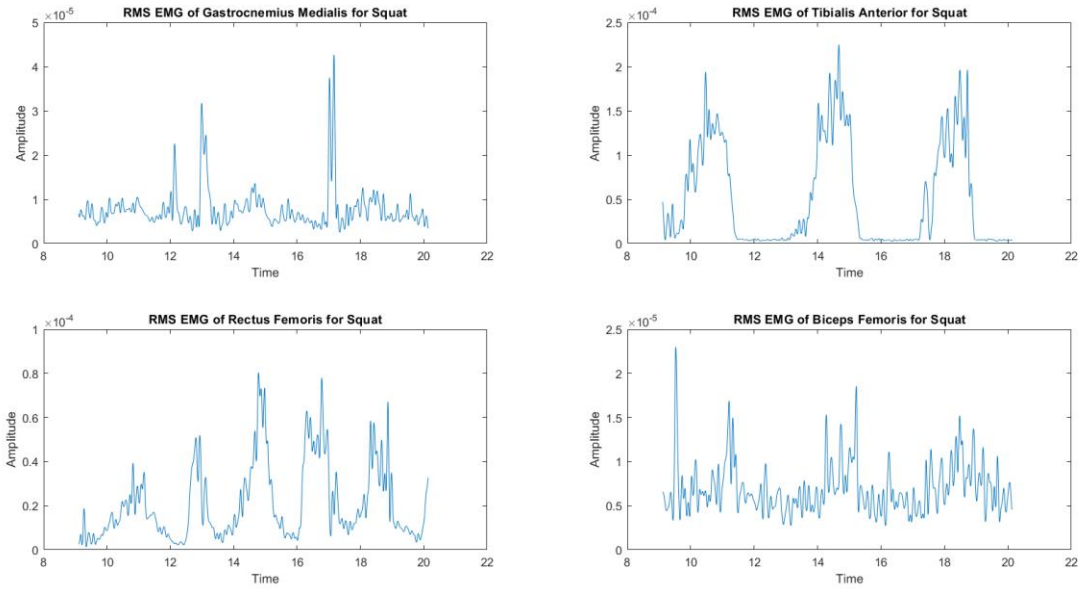

Fig. G.1: RMS EMG data for different muscles during all 3 squat trials in succession. Top left - Gastrocnemius Medialis; Top right - Tibialis Anterior; Bottom Left - Rectus Femoris; Bottom Right - Biceps Femoris.

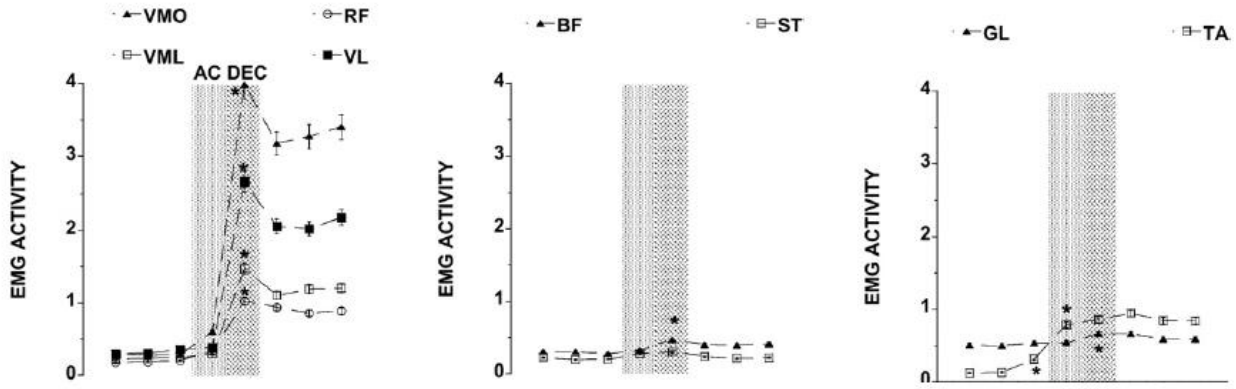

Fig. G.2: EMG activity data for various muscles during the squat, as described by Dionisio *et al*. Important for comparison are the Rectus Femoris (RF), left panel, Biceps Femoris (BF), middle panel, Gastrocnemius Lateralis (GL), right panel, and the Tibialis Anterior (TA), right panel.